

A scalable system for microcalcification cluster automated detection in a distributed mammographic database

Pasquale Delogu^{1,2}, Maria Evelina Fantacci^{1,2}, Alessandro Preite Martinez³, Alessandra Retico², Arnaldo Stefanini^{1,2} and Alessandro Tata²

¹*Dipartimento di Fisica dell'Università di Pisa, Italy*

²*Istituto Nazionale di Fisica Nucleare, Sezione di Pisa, Italy*

³*Centro Studi e Ricerche Enrico Fermi, Roma, Italy*

Abstract

A computer-aided detection (CADE) system for microcalcification cluster identification in mammograms has been developed in the framework of the EU-founded MammoGrid project. The CADE software is mainly based on wavelet transforms and artificial neural networks. It is able to identify microcalcifications in different datasets of mammograms (i.e. acquired with different machines and settings, digitized with different pitch and bit depth or direct digital ones). The CADE can be remotely run from GRID-connected acquisition and annotation stations, supporting clinicians from geographically distant locations in the interpretation of mammographic data. We report and discuss the system performances on different datasets of mammograms and the status of the GRID-enabled CADE analysis.

Keywords: Computer-aided detection, mammography, wavelets, neural networks, GRID applications.

Introduction

The EU-founded MammoGrid project [1] is currently collecting an European-distributed database of mammograms with the aim of applying the emerging GRID technologies [2] to support the early detection of breast cancer. A GRID-based infrastructure would allow the resource sharing and the co-working between radiologists throughout the European Union. In this framework, epidemiological studies, tele-education of young health-care professionals, advanced image analysis and tele-diagnostic support (with and without computer-aided detection) would be enabled.

In the image processing field, we have developed and implemented in a GRID-compliant acquisition and annotation station a computer-aided detection (CADE) system able to identify microcalcifications in different datasets of mammograms (i.e. acquired with different machines and settings, digitized with different pitch and bit depth or direct digital ones).

This paper is structured as follows: the detection scheme is illustrated in sec. 1, sec. 2 describes the database the MammoGrid Collaboration has collected, whereas the tests carried out on different datasets of mammograms and the preliminary results obtained on a set of MammoGrid images are discussed in sec. 3.

1 Description of the CADE system

The CADE procedure we realized is mainly based on wavelet transforms and artificial neural networks. Our CADE system indicates one or more suspicious areas of a mammogram where microcalcification clusters are possibly located, according to the following schema [3]:

- INPUT: digital or digitized mammogram;
- Pre-processing: a) identification of the breast skin line and segmentation of the breast region with respect to the background; b) application of the wavelet-based filter in order to enhance the microcalcifications;
- Feature extraction: a) decomposition of the breast region in several $N \times N$ pixel-wide partially-overlapping sub-images to be processed each at a time; b) automatic extraction of the features characterizing each sub-image;
- Classification: assigning each processed sub-images either to the class of microcalcification clusters or to that of normal tissue;
- OUTPUT: merging the contiguous or partially overlapping sub-images and visualization of the final output by drawing the contours of the suspicious areas on the original image.

1.1 Pre-processing of the mammograms

The pre-processing procedure aims to enhance the signals revealing the presence of microcalcifications, while suppressing the complex and noisy non-pathological breast tissue. A mammogram is usually dominated by the low-frequency information, whereas the microcalcifications appear as high-frequency contributions. Microcalcifications show some evident features at some specific scales, while they are almost negligible at other scales. The use of the wavelet transform [4–6] allows for a separation of the more important high-resolution components of the mammogram from the less important low-resolution ones.

Once the breast skin line is identified, the breast region is processed by the wavelet-based filter, according to the following main steps: identification of the family of wavelets and the level up to which the decomposition has to be performed in order to highlight the interesting details; manipulation of the wavelet coefficients (i.e. suppression of the coefficients encoding the low-frequency contributions and enhancement of those encoding the contributions of interesting details); inverse wavelet transform. By properly thresholding the wavelet coefficients at each level of the decomposition, an enhancement of the microcalcification with respect to surrounding normal tissue can be achieved in the synthesized image. In order to achieve this result, the wavelet basis, the level up to which the decomposition have to be performed and the thresholding rules to be applied to the wavelet coefficients have to be accurately set. All these choices and parameters are application dependent. The size of the pixel pitch and the dynamical range of the gray level intensities characterizing the mammograms are the most important parameters to be taken into account.

1.2 Feature extraction

In order to extract from a mammogram the features to be submitted to the classifier, small regions of a mammogram are analyzed each at a time. The choice of fragmenting the mammogram in small sub-images is finalized both to reduce the amount of data to be analyzed at the same time and to facilitate the localization of the lesions possibly present on a mammogram. The size of the sub-images has been chosen according to the basic rule of considering the smallest squared area matching the typical size of a small microcalcification cluster. Being the size of a single microcalcification rarely greater than 1 mm, and the mean distance between two microcalcifications belonging to the same cluster generally smaller than 5 mm, we assume a square with a 5 mm side to be large enough to accommodate a small cluster. This sub-image size is appropriate to discriminate an isolated microcalcification (which is not considered to be a pathological sign) from a group of microcalcifications close together. The length of the square side in pixel units is obviously determined by the pixel pitch of the digitizer or of the direct digital device. Let us assume that our choice for the length of the square side corresponds to N pixels. In order to avoid the accidental missing of a microcalcification

cluster happening to be at the interface between two contiguous sub-images, we use the technique of the partially overlapping sub-images, i.e. we let the mask for selecting the sub-image to be analyzed move through the mammogram by half of the side length ($N/2$ pixels) at each horizontal and vertical step. In this way each region of a mammogram is analyzed more than once with respect to different neighboring regions.

Each $N \times N$ pixel-wide sub-image extracted from the filtered mammogram is processed by an auto-associative neural network, used to perform an automatic extraction of the relevant features of the sub-image. The implementation of an auto-associative neural network is a neural-based method to perform an unsupervised feature extraction [7–10]. This step has been introduced in the CADe scheme to reduce the dimensionality of the amount of data (the gray level intensity values of the $N \times N$ pixels of each sub-image) to be classified by the system. The architecture of the network we use is a bottle-neck one, consisting of three layers of N^2 input, n hidden (where $n \ll N^2$) and N^2 output neurons respectively. This neural network is trained to reproduce in output the input values. The overall activation of the n nodes of the bottle-neck layer summarize the relevant features of the examined sub-image. The more the $N \times N$ pixel-wide sub-image obtained as output is close to the original sub-image provided as input, the more the activation potentials of the n hidden neurons are supposed to accommodate the information contained in the original sub-image.

It is worth noticing that the implementation of an auto-associative neural network at this stage of the CADe scheme allows for a strong compression of the parameters representing each sub-image ($N^2 \rightarrow n$) to be passed to the following step of the analysis.

1.3 Classification

We use the n features extracted by the auto-associative neural network to assign each sub-image to either the class of sub-images containing microcalcification clusters or the class of those consisting only of normal breast tissue. A standard three-layer feed-forward neural network has been chosen to perform the classification of the n features extracted from each sub-image. The general architecture characterizing this net consists in n inputs, h hidden and two output neurons, and the supervised training phase is based on the back-propagation algorithm.

The performances of the training algorithm were evaluated according to the 5×2 cross validation method [11]. It is the recommended test to be performed on algorithms that can be executed 10 times because it can provide a reliable estimate of the variation of the algorithm performances due to the choice of the training set. This method consists in performing 5 replications of the 2-fold cross validation method [12]. At each replication, the available data are randomly partitioned into 2 sets (A_i and B_i for $i = 1, \dots, 5$) with an almost equal number of entries. The learning algorithm is trained on each set and tested on the other one.

The system performances are given in terms of the sensitivity and specificity values, where the sensitivity is defined as the true positive fraction (fraction of malignant masses correctly classified by the system), whereas the specificity as the true negative fraction (fraction of benign masses correctly classified by the system). In order to show the trade off between the sensitivity and the specificity, a Receiver Operating Characteristic (ROC) analysis has been performed [13, 14]. The ROC curve is obtained by plotting the true positive fraction versus the false positive fraction of the cases ($1 - \text{specificity}$), computed while the decision threshold of the classifier is varied. Each decision threshold results in a corresponding operating point on the curve.

2 The MammoGrid distributed database

One of the main goals of the EU-funded MammoGrid project is the realization of a GRID-enabled European database of mammogram, with the aim of supporting the collaboration among clinicians from different locations in the analysis of mammographic data. Mammograms in the DICOM [15] format are collected through the MammoGrid acquisition and annotation workstations installed in the participating hospitals. Standardized images are stored into the GRID-connected database. The image standardization is realized by the Standard-Mammogram-Form (SMF) algorithm [16] developed by the Mirada Solutions CompanyTM, a partner of the MammoGrid project. The SMF provides a normalized representation of the mammogram, i.e. independent of the data source and of the acquisition technical parameters (e.g. mAs, kVp and breast thickness).

The dataset of fully-annotated mammogram containing microcalcification clusters available at present to CADe developers is constituted by 123 mammograms belonging to 57 patients: 46 of them have been collected and digitized at the University Hospital of Udine (IT), whereas the remaining 11 were acquired by the full-field digital mammography system GE Senographe 2000D at the Torino Hospital (IT); all have been stored in the MammoGrid database by means of the MammoGrid workstation prototype installed in Udine.

3 Tests and results

As the amount of mammograms collected at present in the MammoGrid database is too small for properly training the neural networks implemented in the characterization and classification procedures of our CADe, we used a larger dataset of mammograms for developing the system. Once the CADe has been trained and tested, we adapted it to the MammoGrid images and we evaluated its performances on the MammoGrid database. The dataset used for training and testing the CADe was extracted from the fully-annotated MAGIC-5 database [17]. We used 375 mammograms containing microcalcification clusters and 610 normal

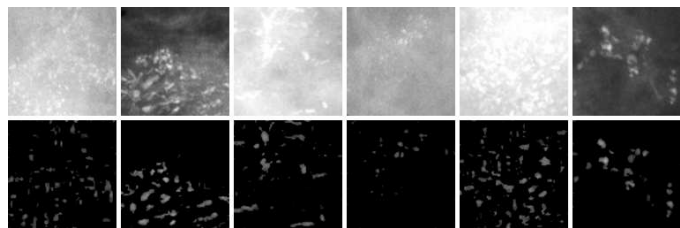


Figure 1: Examples of the wavelet-based filter performances on tissues with different densities (top/bottom: original/filtered sub-images containing microcalcification clusters).

mammograms digitized with a pixel pitch of $85 \mu\text{m}$ and an effective dynamical range of 12 bit per pixel.

3.1 Training and testing the CADe on the MAGIC-5 database

To perform the multi-resolution analysis we considered the Daubechies family of wavelet [4], in particular the db5 mother wavelet. The decomposition is performed up to the fourth level. We found out that the resolution level 1 mainly shows the high-frequency noise included in the mammogram, whereas the levels 2, 3 and 4 contain the high-frequency components related to the presence of microcalcifications. Levels greater than 4 exhibit a strong correlation with larger structures possibly present in the normal breast tissue. In order to enhance microcalcifications, the approximation coefficients at level 4 and the detail coefficients at the first level were neglected. By contrast, the statistical analysis of the distributions of the remaining detail coefficients lead us to keep into account for the synthesis procedure only those coefficients whose values exceed 2σ , where σ is the standard deviation of the coefficient distribution at that level. Some examples of the performance of the filter on mammographic images containing microcalcification clusters embedded in tissues with different densities are shown in fig. 1.

The training and testing of the auto-associative neural network has been performed on a dataset of 149 mammograms containing microcalcification clusters and 299 normal mammograms. The size N of the sub-images to be analyzed by this neural network has been chosen as $N = 60$, thus corresponding to a physical region of $5.1 \times 5.1 \text{ mm}^2$. The number n of units in the hidden layer has been fixed according to the requirement of having the minimum number of neurons allowing for a good generalization capability of the system. Assigning too much neurons to the hidden layer would facilitate the convergence of the learning phase, but it could reduce the generalization capability of the network. Moreover, a too populated hidden layer could set too stringent limits on the minimum number of patterns needed for training the neural classifier implemented in the following step of the analysis. By contrast, a too small hidden layer would lead to the saturation of some of the hidden units and thus negatively affect the overall performance of the system.

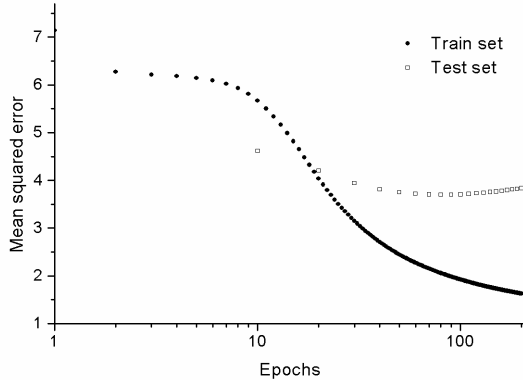


Figure 2: Mean squared errors on the train and test sets in the learning phase of the auto-associative neural network: the minimum error on the test set is reached between 80 and 90 epochs.

A good compromise between these two opposite trends has been reached by assigning 80 units to the hidden layer. The network architecture is thus fixed to be: 3600 input, 80 hidden and 3600 output neurons. The algorithm used in the training procedure is the standard back-propagation with momentum and the activation function is a sigmoid. We used a learning rate of 0.4 and a momentum of 0.2. The behavior of the mean squared error computed during the learning procedure at each epoch on the train set and every ten epochs on the test set is shown in fig. 2. The training phase has been stopped once the error on the test set has reached the minimum value (early stop). As shown in fig. 2 it happens between epochs 80 and 90. The training phase was thus forced to finish in 85 epochs.

The dataset used for the supervised training of the feed-forward neural classifier is constituted by 156 mammograms with microcalcification clusters and 241 normal mammograms. The standard back-propagation algorithm was implemented and the best performance were achieved with 10 neurons in the hidden layer. The performances our learning algorithm achieved according to the 5×2 cross-validation method are reported in tab. 1 in terms of the sensitivity and specificity values. As can be noticed, the performances the neural classifier achieves are robust, i.e. almost independent of the partitioning of the available data into the train and test sets. The average performances achieved in the testing phase are 93.4% for the sensitivity and 91.8% for the specificity.

Once each sub-image of a mammogram has been assigned a degree of suspiciousness, the contiguous or partially-overlapping suspicious sub-images have to be merged in order to evaluate the system performances on the entire mammographic images. A cluster detection criterion has to be *a priori* defined. The effect the choice of the detection criteria in addition to the size of the annotated region has on the CAD performance evaluation have been systematically examined in the literature [18, 19]. As there is no

Table 1: Evaluation of the performances of the standard back-propagation learning algorithm for the neural classifier according to the 5×2 cross validation method.

Train Set	Test Set	Sensitivity (%)	Specificity (%)
A_1	B_1	94.4	91.8
B_1	A_1	92.8	91.1
A_2	B_2	92.3	90.9
B_2	A_2	93.4	92.0
A_3	B_3	92.0	90.5
B_3	A_3	94.5	91.6
A_4	B_4	92.9	93.9
B_4	A_4	94.2	93.0
A_5	B_5	94.6	91.5
B_5	A_5	93.0	91.7

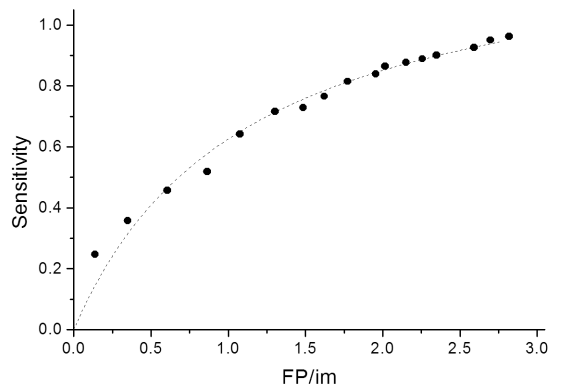


Figure 3: FROC curve obtained on a test set of 140 mammograms (70 containing 89 microcalcifications clusters and 70 normal views) extracted from the MAGIC-5 database.

universal scoring method currently in use for evaluating the performances of a CAD system for microcalcification cluster detection, we briefly describe the detection criteria we adopted:

- a true cluster is considered detected if the region indicated by the system includes two or more microcalcifications located within the associated truth circle;
- all findings outside the truth circle are considered as false positive (FP) detections.

The CADe performances were globally evaluated on a test set of 140 images of the MAGIC-5 database (70 with microcalcification clusters and 70 normal images) in terms of the free-response operating characteristic (FROC) analysis [20] (see fig. 3). The FROC curve is obtained by plotting the sensitivity of the system versus the number of FP detection per image (FP/im), while the decision threshold of the classifier is varied. In particular, as shown in the figure, a sensitivity value of 88% is obtained at a rate of 2.15 FP/im.

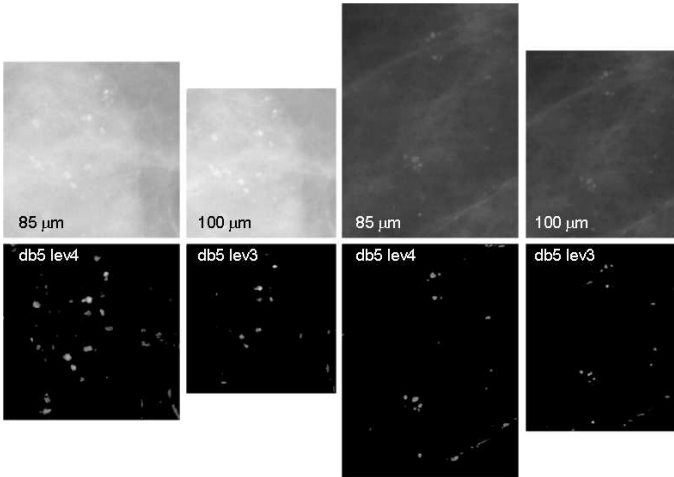


Figure 4: Examples of the performances of the scaling procedure for the CADE filter.

3.2 Testing the CADE on the MammoGrid database

The CADE system we developed and tested on the MAGIC-5 database has been adapted to the MammoGrid SMF images by using the following procedure:

- the wavelet-based filter has been tuned on the SMF mammograms;
- the remaining steps of the analysis, i.e. the neural-based characterization and classification of the sub-images have been directly imported from the MAGIC-5 CADE software.

According to the MammoGrid project work-flow [1], the CADE algorithm has to run on mammograms previously processed by the SMF software [16]. The SMF mammograms are characterized by a different pixel pitch ($100\ \mu\text{m}$ instead of $85\ \mu\text{m}$) and a different effective dynamical range (16 bit per pixel instead of 12) with respect to the MAGIC-5 mammograms. A microcalcification digitized with a $85\ \mu\text{m}$ pixel pitch scanner appears bigger (in pixel units) with respect to the same object digitized with a $100\ \mu\text{m}$ pixel pitch. Therefore, the filter to be applied to the MammoGrid mammograms is required to be sensitive to smaller object. A different choice in the range of scales to be considered in the analysis has proved to be comfortable for accommodating the difference in the pixel pitch. Once the matching of the effective dynamical ranges of the two databases has been performed, the wavelet decomposition is performed up to level 3 instead of 4, being the details at level 4 too big to be correlated to microcalcifications. Only the details at levels 2 and 3 (exceeding 2σ of the experimental distribution) are kept into account for the synthesis. A test of this scaling procedure has been performed on the mammograms of 15 patients acquired both by the MAGIC-5 and by the MammoGrid acquisition workstations. As shown in fig. 4 the matching of the dynamical ranges and the scaling of the wavelet-analysis parameters allows the CADE filter to generate very similar processed images.

The performances the rescaled CADE achieves on the images of the MammoGrid database are the following: a sensitivity of 82.2% is obtained at a rate of 4.15 FP/im. If the analysis is performed independently on the digitized and on the direct digital images, the results are: a 82.1% sensitivity at a rate of 4.8 FP/im in the first case, whereas a 83.3% sensitivity at a rate of 1.6 FP/im in the second case. As can be noticed, the number of FP detection per image in the case of digitized images is appreciably higher with respect to the corresponding rate for the directly digital images. Despite the SMF algorithm performs a sort of normalization of images acquired in different conditions, the digitized images are intrinsically noisier. A comparison with the FROC obtained on the MAGIC-5 database reported in fig. 3 points out that the overall CADE system performances in the case of the MammoGrid database are not as good as those obtained on the MAGIC-5 dataset. One possible explanation for this decrease in sensitivity, is that the MammoGrid database contains already a large number of non-easily detectable cases. In this case an improvement of the CADE performances would be achieved once the database is enlarged.

4 Conclusion

We developed a CADE system for microcalcification cluster identification suitable for different sets of data (digitized or direct digital, acquired with different acquisition parameters, etc.). This CADE system has been developed and tested on the MAGIC-5 database and then adapted to the MammoGrid database of SMF mammograms by re-scaling some of the wavelet-filter parameters. This choice is motivated by two main reasons: the amount of fully-annotated SMF images containing microcalcification clusters available at present to the MammoGrid CADE developers is not large enough to perform a new training of the neural networks implemented in the characterization and classification procedures; moreover, the visual aspect of the filtered sub-images in the case both of MAGIC-5 images and SMF images is actually very similar. This makes us confident that the generalization capability of the neural networks would account for the difference in resolution of the two original datasets. The scaling procedure we developed has two main advantages: the wavelet filter is the only part of the analysis one has to tune on the characteristics of a new dataset, whereas the neural-based characterization and classification procedures do not need to be modified; this scalable system can be tested even on very small databases not allowing for the learning procedure of the neural networks to be properly carried out.

The preliminary results obtained on MammoGrid database are encouraging. Once the planned increase in the population of the database is realized, a complete and more robust test of the CADE performance on the pan-European MammoGrid database would be carried out.

The CADE software is currently available on the GRID-connected acquisition and annotation workstation proto-

types installed in the Hospitals of the MammoGrid Consortium. The CADE can be remotely executed on the distributed database and the clinical evaluation of the CADE as second reader of screening mammograms has already started.

Acknowledgments

This work has been partially supported by the EU-funded MammoGrid project and by the Istituto Nazionale di Fisica Nucleare, Sezione di Pisa, Italy.

References

- [1] The Information Societies Technology project: MammoGrid - A European federated mammogram database implemented on a GRID infrastructure, EU Contract *IST-2001-37614*.
- [2] I. Foster and C. Kesselman, The Grid: Blueprint for a New Computing Infrastructure, Morgan Kaufmann publishers, 1998. ISBN 1558604758.
- [3] P. Delogu, M.E. Fantacci, A. Preite Martinez, A. Retico, A. Stefanini and A. Tata, A scalable Computer-Aided Detection system for microcalcification cluster identification in a pan-European distributed database of mammograms, accepted for publication on *Nucl. Instrum. Meth. A* (estimated publication month April 2006).
- [4] I. Daubechies, Ten Lectures on Wavelets, *SIAM* Philadelphia 1992.
- [5] Y. Meyer, Wavelets: Algorithms and Applications, *SIAM* Philadelphia 1993.
- [6] S.G. Mallat, A theory for multi-resolution signal decomposition, *IEEE Trans. Pattern Anal. Machine Intell.* **11**, 674–693, 1989.
- [7] M.A. Kramer, Non linear principal components analysis using auto-associative neural networks, *AICHE J* **37**, 233–243, 1991.
- [8] M.A. Kramer, Auto-associative neural networks, *Comput. Chem. Eng.* **16**, 313–328, 1992.
- [9] J.A. Leonard and M.A. Kramer, Diagnosing dynamic faults using modular neural nets, *IEEE Expert* **8**, 44–53, 1993.
- [10] D.R. Kuespert and T.J. McAvoy, Knowledge extraction in chemical process control, *Chem. Eng. Comm.* **130**, 251–264, 1994.
- [11] T.G. Dietterich, Approximate Statistical Test For Comparing Supervised Classification Learning Algorithms, *Neural Computation* **10**(7), 1895–1923, 1998.
- [12] M. Stone, Cross-validatory choice and assessment of statistical predictions, *J Royal Statistical Soc. B* **36**, 111–147, 1974.
- [13] C.E. Metz, ROC methodology in radiologic imaging, *Invest. Radiol.* **21**(9), 720–733, 1986.
- [14] J.A. Hanley and B.J. McNeil, The meaning and use of the area under a receiver operating characteristic (ROC) curve, *Radiology* **143**(1), 29–36, 1982.
- [15] Digital Imaging and Communications in Medicine (DICOM). See <http://medical.nema.org/>
- [16] Standard Mammogram Form (SMF), Mirada Solutions™, <http://www.mirada-solutions.com/smf.htm>.
- [17] R. Bellotti et al., The MAGIC-5 Project: Medical Applications on a Grid Infrastructure Connection, *Proc IEEE NSS Conf. Rec.* **3**, 1902–1906, 2004.
- [18] G. te Brake and N. Karssemeijer, Detection Criteria for Evaluation of the Computer Aided Diagnosis Systems, *18th Annual International Conference of the IEEE Engineering in Medicine and Biology Society* 1996.
- [19] Kallergi M, Carney GM and Gaviria J, Evaluating the performance of detection algorithms in digital mammography, *Med Phys* 1999 **26**(2) pp 267–75.
- [20] D. Chakraborty, Free-response methodology: Alternative analysis and a new observer-performance experiment, *Radiology* **174**(3), 873–881, 1990.